

ON THE GENERALIZED KRAMERS PROBLEM WITH OSCILLATORY MEMORY FRICTION

Ramón Reigada

Department of Chemistry and Biochemistry 0340
University of California San Diego
La Jolla, California 92093-0340

and

Departament de Química Física
Universitat de Barcelona
Av. Diagonal 647, E-08028 Barcelona, Spain

Aldo H. Romero

Department of Chemistry and Biochemistry 0340
and Department of Physics
University of California, San Diego
La Jolla, California 92093-0340

Katja Lindenberg

Department of Chemistry and Biochemistry 0340
and Institute for Nonlinear Science
University of California San Diego
La Jolla, California 92093-0340

José M. Sancho

Departament d'Estructura i Constituents de la Matèria
Universitat de Barcelona
Av. Diagonal 647, E-08028 Barcelona, Spain

October 13, 2018

Abstract

The time-dependent transmission coefficient for the Kramers problem exhibits different behaviors in different parameter regimes. In the high friction regime it decays monotonically (“non-adiabatic”), and in the low friction regime it decays in an oscillatory fashion (“energy-diffusion-limited”). The generalized Kramers problem with an exponential memory friction exhibits an additional oscillatory behavior in the high friction regime (“caging”). In this paper we consider an oscillatory memory kernel, which can be associated with a model in which the reaction coordinate is linearly coupled to a nonreactive coordinate, which is in turn coupled to a heat bath. We recover the non-adiabatic and energy-diffusion-limited behaviors of the transmission coefficient in appropriate parameter regimes, and find that caging is not observed with an oscillatory memory kernel. Most interestingly, we identify a new regime in which the time-dependent transmission coefficient decays via a series of rather sharp steps followed by plateaus (“stair-like”). We explain this regime and its dependence on the various parameters of the system.

1 Introduction

The classic Kramers formulation of reaction rates in solution [1] and its generalization to non-Markovian solvents [2] has provided many theoretical challenges over the past six decades [3–6]). In this formulation the reaction coordinate $x(t)$ is modeled as evolving in a double-well potential $V(x)$ with a barrier separating the reactant and product states. The solvent effects are modeled in terms of fluctuating and dissipative forces. A full understanding of the dependence of the rate coefficient k on the dissipation in the Markovian solvent limit (the “turnover problem”) has only been achieved in the last few years [4, 7, 8]. Comparably thorough understanding in the case of a non-Markovian solvent is not yet available. Understanding of the temperature dependence of k is also far from complete [9–12]. Clearly, there is yet a great deal to learn about this classic problem.

In the past two decades, and most especially in the past few years, attention has also been paid by a number of investigators to the time-dependence of the rate coefficient, that is, the way in which $k(t)$ approaches its asymptotic value $k(\infty)$ [11–16]. This time dependence directly mirrors the dynamics of the reaction coordinate in the barrier region on the way toward capture by one well or the other. Our focus is on this time dependence and the way that it is influenced by the parameters of the system.

The generalized Kramers problem is based on the dynamical equations for the reaction coordinate

$$\ddot{x} = - \int_0^t dt' \Gamma(t-t') \dot{x}(t') - \frac{dV_{eff}(x)}{dx} + F(t), \quad (1)$$

where a dot denotes a time derivative, $V_{eff}(x)$ is an effective potential related to $V(x)$ (cf. next section), $\Gamma(t-t')$ is the dissipative memory kernel (which we will often simply call the *memory kernel*), and $F(t)$ represents Gaussian fluctuations that satisfy the fluctuation-dissipation relation

$$\langle F(t)F(t') \rangle = k_B T \Gamma(t-t'). \quad (2)$$

The brackets $\langle \dots \rangle$ denote an ensemble average, k_B is Boltzmann’s constant, and T is the temperature. The fluctuations and dissipation account for the interaction of the reaction coordinate with the surrounding medium. The original Kramers problem dealt with a Markovian solvent, that is, with instantaneous dissipation:

$$\Gamma(t) = 2\gamma\delta(t). \quad (3)$$

The parameter γ is the dissipation parameter or damping parameter. Generalizations to the non-Markovian problem have typically focused on exponential memory kernels [2],

$$\Gamma(t) = \frac{\gamma}{\tau} e^{-t/\tau}, \quad (4)$$

and on oscillatory memory kernels [2],

$$\Gamma(t) = \Gamma(0) e^{-t/\tau} \left(\cos \Omega t + \frac{1}{\Omega\tau} \sin \Omega t \right) \quad (5)$$

(this memory kernel and the parameters in it will be discussed in detail in the next section). Another generalization, which we do not address in our work, deals with Gaussian memory

kernels [2, 15],

$$\Gamma(t) = \left(\frac{2}{\pi}\right)^{1/2} \frac{\gamma}{\tau} e^{-t^2/2\tau^2}. \quad (6)$$

In all of these generalizations τ is a measure of the decay time of the memory kernel or, equivalently, of the correlation time of the fluctuations.

In subsequent sections we will provide a brief graphic review of the results addressed in our previous work, which succinctly are as follows. The time-dependent rate coefficient for the Markovian solvent at high damping (that is, beyond the “turnover” regime) decays monotonically towards its equilibrium value [16]. For the exponential memory at high damping there are *two* distinct types of time dependences, the “non-adiabatic”, in which the rate coefficient decays monotonically to its equilibrium value (as in the Markovian case), and the “caging”, in which the decay to equilibrium is oscillatory with a frequency characteristic of an effective caging potential [16]. At very low damping (that is, below the “turnover”), the decay of the rate coefficient to its equilibrium value is again oscillatory, but now with a frequency characteristic of the bistable potential. This behavior is apparent for the Markovian solvent [11] and also for the exponential memory [12] in this energy-diffusion-limited regime. We have shown that the theoretical predictions agree very well with numerical simulations for all of these generic behaviors.

In this paper we complete our analysis with a study of the oscillatory memory kernel. In appropriate limits we recover the typical low-damping behavior of the rate coefficient and also the high-damping non-adiabatic monotonic behavior, although caging, as we will see, can not be achieved with an oscillatory memory. Most interesting, perhaps, is the appearance of a new time dependence different from those previously observed or anticipated. This new time dependence is a consequence of the new features of the memory kernel such as the fact that it alternates between positive and negative values. We will present and explain this new behavior, and determine the parameter regimes where it may be observed.

This paper is organized as follows. In Sec. 2 we introduce the model Eq. (1) in detail. In fact, we present two equivalent versions of the model. One version invokes a solvent coordinate which is coupled to the reaction coordinate and also coupled to a heat bath. This double presentation not only clarifies the physical origin of the oscillatory memory kernel, but it also leads to more transparent interpretation of the resulting time dependence of the rate coefficient. In Sec. 3 we describe our simulations and numerical procedures. Section 4 presents a graphical summary of the various time dependences obtained numerically in earlier work and provides a context for the presentation of the new behavior identified in the oscillatory memory system. In Sec. 5 we discuss analytic approximations that serve as a backdrop for our analysis and detailed explanation of the new behavior, which is presented in Sec. 6. The results and conclusions are summarized in Sec. 7.

2 The Model

We first present an alternative (two-variable) model that eventually leads to Eq. (1) with Eq. (5). The potential energy of the two-variable model is

$$V(x, y) = V(x) + \frac{\omega^2}{2} y^2 + \frac{k}{2} (x - y)^2, \quad (7)$$

where the solvent is explicitly represented by a harmonic coordinate y . The reaction coordinate x evolves in a bistable potential that is taken to be of the familiar form

$$V(x) = \frac{V_0}{4}(x^2 - 1)^2. \quad (8)$$

We take V_0 as the energy unit throughout this work and thus set it equal to unity. The reaction coordinate is coupled to the solvent coordinate via a harmonic spring of force constant k . The dynamical equations for the coupled system, assuming that y is coupled to a heat bath at temperature T , are

$$\begin{aligned} \ddot{x} &= -\frac{dV(x)}{dx} + k(y - x), \\ \ddot{y} &= -\omega^2 y + k(x - y) - \gamma \dot{y} + f(t). \end{aligned} \quad (9)$$

Here γ is the friction coefficient for the solvent coordinate and $f(t)$ represents δ -correlated Gaussian fluctuations that satisfy the fluctuation-dissipation relation

$$\langle f(t)f(t') \rangle = 2\gamma k_B T \delta(t - t'). \quad (10)$$

Throughout we take the barrier height to be large compared to the temperature, $k_B T \ll 1/4$. We call Eq. (9) the “extended” representation of our system.

Although the extended model can readily be integrated numerically, initial conditions are not arbitrary and require careful consideration. The reduction of the model (9) to the generalized Kramers problem (1) with the fluctuation-dissipation relation (2) requires distributions for the initial solvent coordinate $y(0)$ and velocity $\dot{y}(0)$ that satisfy certain conditions (cf. Appendix A, where these initial conditions are presented in detail).

A number of theoretical approaches to this problem deal, instead, with the completely equivalent “contracted” or “reduced” representation obtained by explicitly integrating out the solvent coordinate y . Among these is the work of Grote and Hynes [2] and that of Kohen and Tannor (KT) [16]. The resulting equivalent single-variable problem is shown in Appendix A to be given by Eq. (1) with the effective potential

$$V_{eff}(x) = V(x) + \frac{1}{2} \frac{\omega^2 k}{\omega^2 + k} x^2. \quad (11)$$

Depending on the relative values of parameters, the resulting memory kernel can decay monotonically (“hyperbolic” case) or it can decay in an oscillatory fashion (“trigonometric” case). We are specifically interested in the trigonometric case, which requires that

$$\left(\frac{\gamma}{2}\right)^2 - \omega^2 - k < 0. \quad (12)$$

The associated memory kernel is

$$\Gamma(t) = \frac{k^2}{\omega^2 + k} e^{-\frac{\gamma}{2}t} \left(\frac{\gamma}{2\Omega} \sin \Omega t + \cos \Omega t \right) \quad (13)$$

with the frequency

$$\Omega \equiv \sqrt{\omega^2 + k - \left(\frac{\gamma}{2}\right)^2}. \quad (14)$$

We expect that the oscillatory character of the memory kernel may lead to new regimes of dynamical behavior that will become evident in the time dependence of the rate coefficient. We do not pursue the hyperbolic case because we expect behavior similar to that found earlier for the exponential memory kernel and hence do not expect new behaviors in this case.

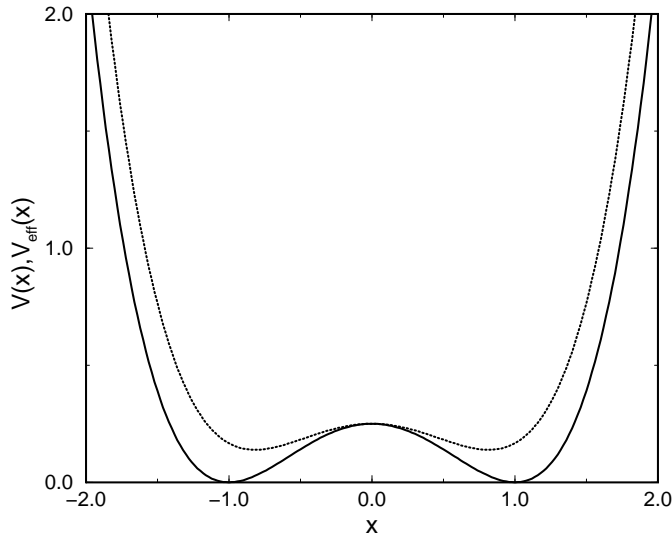


Figure 1: Solid line: original bistable potential $V(x)$ of Eq. (8). Dotted line: effective potential $V_{eff}(x)$ of Eq. (11) for $\omega^2 = 0.5$ and $k = 1$.

From the explicit form (11) of the effective potential we see that the additional quadratic term moves the minima of the wells of the bistable potential $V(x)$ from ± 1 to

$$x_{min} = \pm \sqrt{1 - \frac{\omega^2 k}{\omega^2 + k}} \quad (15)$$

and diminishes the barrier from $1/4$ to

$$\Delta V_{eff}^\ddagger = \frac{1}{4} - \frac{1}{2} \left(\frac{\omega^2 k}{\omega^2 + k} \right) + \frac{1}{4} \left(\frac{\omega^2 k}{\omega^2 + k} \right)^2. \quad (16)$$

Both effects can be seen in Fig. 1. It is easily shown that the barrier disappears entirely when $\omega^2 k \geq \omega^2 + k$, at which point the very nature of the problem changes. We thus constrain our parameters k and ω^2 to ensure bistability:

$$\omega^2 k < \omega^2 + k. \quad (17)$$

To summarize, then, the model to be considered in this paper is given by Eqs. (9) with

the potential (8) and the fluctuation-dissipation relation (10) (extended representation), or, completely equivalently, by Eq. (1) with the effective potential (11), the memory kernel (13), and the fluctuation-dissipation relation (2) (reduced representation). Whichever formulation is used, our parameters are constrained by the inequality (17), which ensures a bistable effective potential, and by the inequality (12), which ensures an oscillatory memory kernel. For some purposes the extended representation provides a more convenient viewpoint, while for others the reduced representation is more transparent. In particular, we find the extended representation more convenient for numerical simulations.

As a final point in this section it is important to note the altered significance of parameters in the oscillatory memory kernel compared to the Markovian or exponential models. In the latter two cases “high friction” and “low friction” refer to the value of γ since this parameter directly measures the strength of the dissipative force that extracts energy from the reaction coordinate into the bath. Thus, in the exponential memory case γ is the value of $\Gamma(0)$ and also of the integrated memory kernel. In the case under consideration here, however, γ is a measure of the dissipative force on the *solvent* coordinate and not directly on the reaction coordinate. Although γ indirectly affects the loss of energy of the reaction coordinate, the energy loss channel is now principally determined by the coupling strength between the reaction coordinate and the solvent coordinate. Correspondingly, now $\Gamma(0) = k^2/(\omega^2 + k)$. The integrated memory kernel is $\Gamma(0)\gamma/(\omega^2 + k)$, thus reflecting the overall influence of γ . However, it is the coupling constant k that now essentially determines whether we are in the “high friction” or “low friction” regime (more details will be presented in Sec. 4).

3 Simulation Method: Initial Conditions and Other Details

The quantity of interest is the time-dependent rate coefficient $k(t)$ for an ensemble of particles evolving according to $x(t)$ in Eq. (1) or Eq. (9). Numerically we find it more convenient to work with the extended system (9). The coefficient $k(t)$ is the time-dependent mean rate of passage of the particles across the barrier at $x = 0$. The usual focus on the deviation of $k(t)$ from its equilibrium transition state theory (TST) value [3,4,11] leads to the expression

$$k(t) = \kappa(t)k^{TST} \quad (18)$$

where $k^{TST} = (\sqrt{2}/\pi) \exp(-1/4k_B T)$ is the transition state theory rate that assumes that particles never recross the barrier. The transmission coefficient $\kappa(t)$ is the correction to transition state theory that includes both the temporal dynamics and the effects of those particles that do recross the barrier. We are interested in the dynamics of the transmission coefficient $\kappa(t)$.

Numerically, one might try to calculate $k(t)$ directly by starting all the particles in one well and computing at each time how many of them have crossed to the other well. It would require an exceedingly long calculation to gather statistically significant data in this manner, since the reaction barrier is very much higher than the thermal fluctuations. The reactive flux formalism [3,17,18] that relies on Eq. (18) overcomes this difficulty since the transmission coefficient can be calculated by dealing only with an ensemble of particles whose initial position is above the barrier [$x(0) = 0$]. The slow process of “getting there” is already included in k^{TST} . Half of the particles that start above the barrier have a positive velocity distributed according to the Boltzmann distribution in energy, and the other half have the same distribution but with negative velocities.

Upon imposing the initial conditions on y discussed in Appendix A, we run quite a few iterations for the solvent coordinate evolution in order to obtain even better thermalization. Having achieved this, we then integrate the fully coupled system (9) with the following distributions for the initial reaction coordinate position $x(0) \equiv x_o$ and initial velocity $\dot{x}(0) \equiv v_{x_o}$:

$$P(x_o) = \delta(x_o), \quad (19)$$

$$P(v_{x_o}) = \frac{v_{x_o}}{k_B T} \exp\left(-\frac{v_{x_o}^2}{2k_B T}\right). \quad (20)$$

The numerical integration is carried out using the second order Heun's algorithm [19,20]. In all our runs our ensemble consists of $N = 10,000$ particles and we use a very small time step ($\Delta t = 0.001$). The transmission coefficient is calculated from these simulated data according to the relation [17]

$$\kappa(t) = \frac{N_+(t)}{N_+(0)} - \frac{N_-(t)}{N_-(0)}, \quad (21)$$

where $N_+(t)$ and $N_-(t)$ are the particles that started with positive velocities and negative velocities respectively and at time t are in or over the right hand well (i.e., the particles for which $x(t) > 0$). Alternatively and completely equivalently (via a simple symmetry argument) one can start all the x particles with a positive velocity and then

$$\kappa(t) = \kappa_+(t) - \kappa_-(t) \quad (22)$$

where $\kappa_+(t)$ is the fraction of particles that are in or over the right hand well at time t , and $\kappa_-(t)$ is the fraction in or over the left hand well. Furthermore, it is easily argued that [11]

$$\kappa_-(t) = 1 - \kappa_+(t), \quad (23)$$

so it is sufficient to follow one or the other.

4 Numerical Results

The number of independent parameters in the generalized Kramers problem with an oscillatory memory kernel is of course larger than for Markovian or exponential frictions. The values of $\kappa(t)$ and κ_{st} now in general depend on k , ω^2 , γ , and $k_B T$. Indeed, a systematic, even qualitative study of the transmission coefficient as was done, for example, in [11,12] would be quite complex. We focus on a more modest goal, that is, to capture qualitatively the different types of temporal behavior of $\kappa(t)$ and the broad parameter regimes where each occurs. These include the three regimes identified for the exponential memory, namely, the energy-diffusion-limited, the non-adiabatic, and the caging regimes, as well as possible new behaviors.

The oscillatory memory kernel can exhibit different appearances depending on the parameter choices. Figure 2 exhibits three distinct ‘‘generic’’ appearances, each roughly representative of a distinct parameter regime. Two of these mimic behaviors of the exponential memory kernel and might be expected to lead to transmission coefficients similar to those

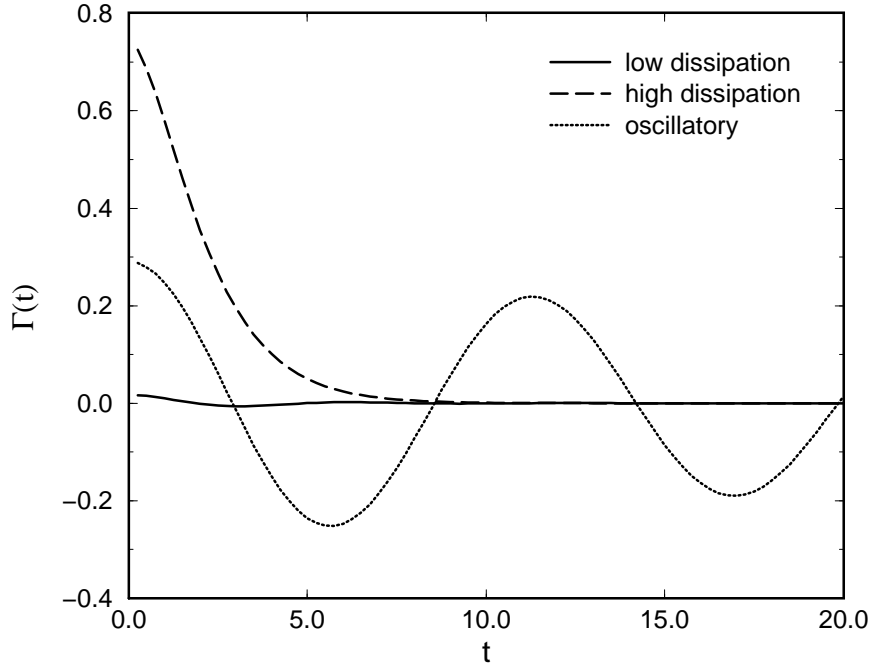


Figure 2: Memory kernel $\Gamma(t)$ vs t for the different regimes studied in Sec. 4. Solid curve: $\omega^2 = 1.0$, $k = 0.14$, and $\gamma = 0.667$. Dashed curve: $\omega^2 = 0.01$, $k = 0.75$, and $\gamma = 1.74$. Dotted curve: $\omega^2 = 0.01$, $k = 0.3$, and $\gamma = 0.05$.

obtained earlier. The third, the strongly oscillatory kernel, is new and might be expected to lead to new behavior. Let us consider each case in turn, along with the resulting transmission coefficients.

The solid curve kernel in Fig. 2 mimics the exponential memory kernel in the energy-diffusion-limited regime. The kernel $\Gamma(t)$ is small at all times. In the case of the exponential memory kernel (4) this behavior was insured by choosing γ to be small, but in the oscillatory memory case, as noted earlier, the meaning of the parameters is different. Now a small value of $\Gamma(t)$ and, in particular, a small value of $\Gamma(0)$ is insured if we choose small values of $k^2/(\omega^2 + k)$, that is, k must be small and/or ω^2 must be large. Note that the choices must still obey the constraint (17), but this is not a problem. The value of γ is not constrained by the low friction requirement, but it *is* constrained by Eq. (12) if we want to insure that we are in the oscillatory regime. The value of γ determines the oscillation frequency of the memory kernel $\Gamma(t)$ but not its magnitude.

Typical values of the parameters that satisfy the conditions to produce energy-diffusion-limited behavior while preserving the oscillatory character of the memory kernel are $\omega^2 = 1.0$, $k = 0.14$, and $\gamma = 0.667$. These are the values used to produce the solid curve in Fig. 2. In this regime the low dissipation causes the dynamics of the system to be dominated by the slow variation of the energy and consequently by the repeated inertial recrossing of the barrier before the particles are trapped in one well or the other. As expected, we find the typical energy-diffusion-limited behavior for $\kappa(t)$ (oscillatory curve in Fig. 3) that consists of a very small initial decay to a plateau up to a time beyond which $\kappa(t)$ decays

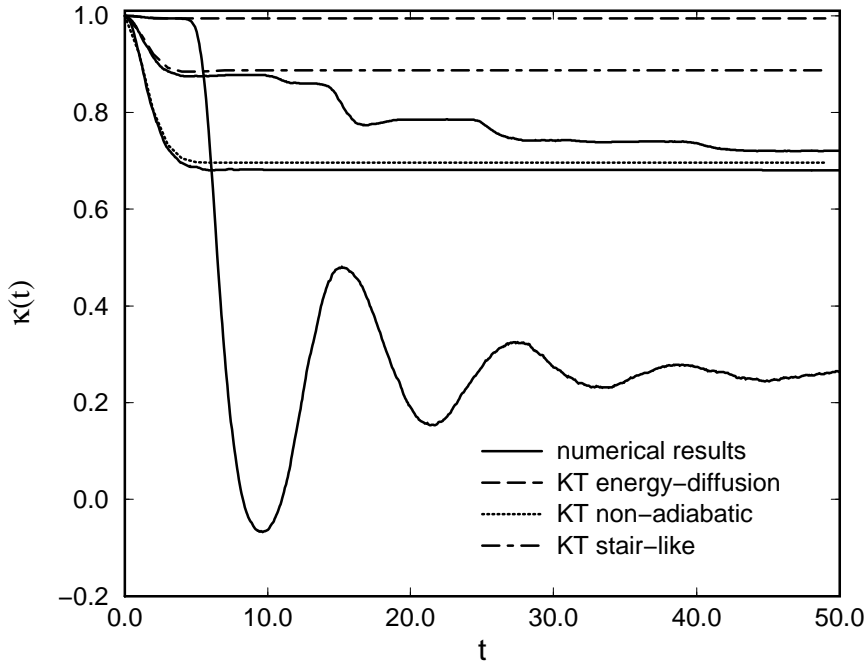


Figure 3: Solid curves: the three typical behaviors of the transmission coefficient with oscillatory memory friction (numerical results). Oscillatory curve: $\omega^2 = 1.0$, $k = 0.14$, and $\gamma = 0.667$ (energy-diffusion-limited regime). Monotonic curve: $\omega^2 = 0.01$, $k = 0.75$, and $\gamma = 1.74$ (non-adiabatic regime). The temperature for these two cases is $k_B T = 0.025$. Stepped curve: $\omega^2 = 0.01$, $k = 0.3$, and $\gamma = 0.05$ (new “stair-like” regime). The temperature is $k_B T = 0.015$. The dotted, dashed, and dot-dashed curves correspond to the KT theory results for the same parameter values.

in an oscillatory manner to its equilibrium value. As shown and discussed in our earlier work [11,12], the first decay is due to the few low-energy particles that immediately change their initial direction due to a thermal fluctuation and are trapped in the well opposite to the one toward which they were initially moving. The oscillations are associated with the essentially inertial successive recrossings of the higher-energy particles.

All the arguments developed in the reduced system should have a counterpart in the extended scheme. In the energy-diffusion-limited case we have considered small k , large ω^2 , and arbitrary γ [subject to the constraint (12)]. Large ω^2 leads to a narrow harmonic potential for y [and consequently $y(t)$ remains small], and small k means weak coupling. Since the coupling term ky in Eqs. (9) provides the only energy loss channel for the x coordinate, large ω^2 and small k therefore lead to low dissipation.

Let us now move on to the high dissipation regime. The dashed curve in Fig. 2 mimics the exponential memory kernel in the diffusion-limited regime. The kernel $\Gamma(t)$ has a high initial value and decays essentially monotonically (although we *are* in the oscillatory regime). In the case of the exponential memory kernel (4) this regime results when γ is large. For the exponential memory kernel, the choice of the second parameter, τ , further determines two different regimes of behavior. If the correlation time τ is small, such that $\gamma/\tau < 1$,

the transmission coefficient decays monotonically and one is said to be in the non-adiabatic regime. This is also the unique high-dissipation behavior associated with the Markovian problem. On the other hand, if τ is small, such that $\gamma/\tau > 1$, one is in the caging regime in which the behavior of the transmission coefficient is oscillatory (but quite differently so than in the low dissipation regime). The quasi-exponential dashed memory kernel in Fig. 2 corresponds to the non-adiabatic behavior since the ratio of the initial value (about 0.8) to the decay time of the kernel (about 4.0) is clearly smaller than unity. In order to have the oscillatory memory mimic the non-adiabatic exponential memory case as in the figure we require γ to be *small* (since now γ plays the role that $1/\tau$ did before), and Ω to be small as well (to minimize oscillatory effects). A typical set of values that meets these various conditions is $\omega^2 = 0.01$, $k = 0.75$, and $\gamma = 1.74$, which leads to $\Omega = 0.0557$.

The associated transmission coefficient for these parameters exhibits the typical features of the non-adiabatic regime, as shown by the monotonic curve in Fig. 3, namely, a smooth rather rapid decay to the equilibrium value. As in the case of an exponential memory, this decay in the non-adiabatic regime looks Gaussian rather than exponential at short times.

In the extended system small ω^2 means that the potential in y is very wide and for this reason $y(t)$ easily achieves large values. Large k represents strong coupling, and the combination of both conditions leads to high dissipation for the x coordinate.

As noted above, the other regime found for an exponential memory kernel with high dissipation is the caging regime, which there occurs when both γ and τ are large, with $\gamma/\tau > 1$. Interestingly, the constraints on the parameters and the shape of the oscillatory friction kernel do not admit this regime. This can be understood from the following argument. Caging is achieved when $\Gamma(t)$ is essentially constant over some substantial time range so that the friction integral in Eq. (1) over this time can be approximated as a linear force on $x(t)$ and such that the resulting potential becomes monostable. In our case, this resulting potential $V_r(x)$ would be

$$V_r(x) = \frac{1}{4}(x^2 - 1)^2 + \frac{1}{2} \frac{\omega^2 k}{\omega^2 + k} x^2 + \frac{1}{2} \frac{k^2}{\omega^2 + k} x^2 = \frac{1}{4}(x^2 - 1)^2 + \frac{1}{2} k x^2. \quad (24)$$

From this expression it is easy to deduce that the potential $V_r(x)$ loses its barrier when $k > 1$. The combination of the condition that $\Gamma(t)$ behave roughly as a constant for some time interval (γ small) and that the resulting potential lose its barrier during this time ($k > 1$) would lead to a caging regime with effective caging potential frequency $\omega_{cag} = \sqrt{k - 1}$. However, this combination of conditions can not be satisfied with an oscillatory memory. If we increase the value of k above 1, we also have to increase γ (Ω has to remain small to avoid pronounced oscillations), but this in turn leads to the rapid exponential decay of $\Gamma(t)$. It is thus not possible to achieve the conditions for the caging regime with trigonometric oscillatory friction. The caging regime is easily captured in the hyperbolic case (cf. Appendix A), since then $\Gamma(t)$ can take on a very high initial value that can be sustained for a long time.

We have thus seen that the form of $\Gamma(t)$ and the constraints on k , ω^2 , and γ determine which regimes typical of exponential memories can also be captured with an oscillatory memory. The requirements described so far have been met by either choosing $\Gamma(0)$ to be small (low dissipation) or large (high dissipation) while minimizing the amplitude of the oscillations.

New behaviors for the dynamics of $\kappa(t)$ may appear in parameter regimes that emphasize the oscillatory behavior of $\Gamma(t)$. To provide such emphasis we minimize the damping effects

of the exponential part by choosing γ to be small. Further choosing a very small value for ω^2 and a medium value for k (large enough to get high amplitudes of oscillation of $\Gamma(t)$, but limited so that the frequency Ω is not too high) we obtain the oscillatory friction shown as the dotted kernel in Fig. 2. Since γ and ω^2 are very small, the frequency of the oscillations is

$$\Omega \approx \sqrt{k}. \quad (25)$$

In this regime at low temperatures an entirely new temporal behavior emerges for $\kappa(t)$. We generically call this the “stair-like” regime. It is shown for a typical set of parameter values in Fig. 3 (corresponding to those of the dotted curve in Fig. 2). The main feature of this new behavior is that $\kappa(t)$ exhibits a “stair” shape, namely, it decays via a series of steps followed by plateaus. The explanation of this behavior, including the period of the steps, the dependences on the parameters γ , ω^2 , k , and $k_B T$, and the connections with the other regimes are presented in detail in Sec. 6.

5 Approximations

In this section we lay the groundwork for the arguments invoked in the next section, where we discuss the stair-like regime in detail. Our explanations are semi-quantitative, that is, we do not develop a theory that reproduces the stair-like curve in the figure in all its details. We mention this because in fact such theories *are* available for the two other curves [11, 12, 14, 16]. In the high dissipation regime the KT theory predicts the monotonic decay in the non-adiabatic regime, and this prediction, shown in Fig. 3, is seen to be quantitatively very good (see also [11, 12]). In the low dissipation regime we have shown that our theory also leads to very good quantitative agreement with numerical results for the entire time evolution of $\kappa(t)$ [11, 12]. We have not derived such a detailed formula for the stair-like regime, but we nevertheless have been able to gain considerable understanding of this behavior, and this is what we shall present.

Our insights turn out to be most complete if we invoke both representations of the oscillatory problem, the extended as well as the reduced. Furthermore, an understanding of the early time dependence of $\kappa(t)$ in both of these representations turns out to be very helpful, even if the approximations that are invoked are not valid over the entire time regime – the breakdown of approximations can also yield useful insights. We thus first turn to the early time behavior.

Consider first the reduced representation. KT theory focuses on the way in which particles subject to dynamics of the generic form (1) with the potential approximated by a parabolic barrier diffuse to one side or the other of the barrier. Since their analysis is restricted to a parabolic barrier (rather than a bistable potential), the theory is appropriate only for high dissipation, that is, when the reaction coordinate never recrosses the barrier once it has left the barrier region. In other cases KT theory may (and indeed does) capture only the initial decay, typically up to the first plateau value of $\kappa(t)$, but it does not capture the asymptotic values κ_{st} . This is seen in Fig. 3, where the KT theory predictions are shown for each of the generic transmission coefficients. KT theory works very well for all times for the non-adiabatic high dissipation curve, and captures the initial decay in the energy-diffusion-limited (dashed curve) and stair-like (dot-dashed curve) cases. These initial agreements are fairly typical for all parameter values.

Consider now the extended representation (9). We introduce an even simpler approxi-

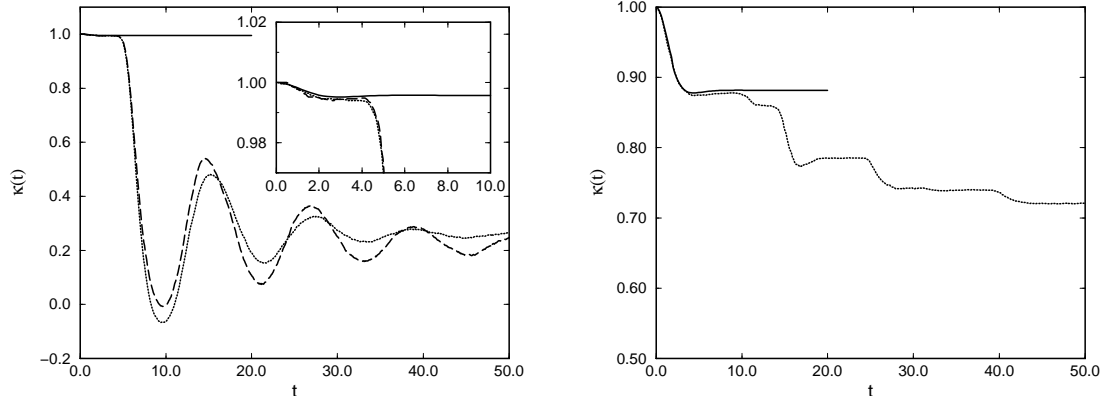


Figure 4: Left panel: The dotted and dashed curves are numerical simulations of the transmission coefficient $\kappa(t)$ vs t in the energy-diffusion-limited regime. In both cases $\omega^2 = 1.0$, $k = 0.14$ and $k_B T = 0.025$. Dotted curve: $\gamma = 0.667$ (same value as in Fig. 3); dashed curve: $\gamma = 0.05$. The solid line, which reproduces both early time behaviors very closely (see inset), is obtained from our early-time approximation for the extended system, Eq. (26). Right panel: the dotted curve is our simulation in the stair-like regime (cf. Fig. 3). The solid curve is the early-time approximation.

mation in this representation that also captures the early time behavior when the dissipation of energy in the x -coordinate is slow and that facilitates our analysis of the stair-like regime. The approximation is based on three main assumptions, all appropriate only at short times. One is akin to the argument we used earlier in the energy-diffusion-limited problem, namely, that the main influence of the temperature arises from the initial thermal distributions. Thus, as long as the initial distributions are chosen correctly, that is, according to Eqs. (A6), (A7), (19), and (20), the thermal effects in the form of the explicit random force acting on the solvent coordinate can be omitted from the dynamical equations. The second is the omission of the dissipation term, i.e., we set γ to zero. Note that this is the dissipative force on the solvent coordinate; the principal initial dissipative channel for the reaction coordinate $x(t)$ is its coupling to the y coordinate via k , and this is retained. The third is to use a parabolic barrier to approximate the potential. With these assumptions the initial decay of the transmission coefficient is due to the low-energy particles (i.e. those barely above the barrier) that are pulled by the y coordinate in a direction opposite to the one indicated by their initial velocity, as described by the simplified deterministic coupled linear equations

$$\begin{aligned}\ddot{x}(t) &= (1 - k)x + ky \\ \ddot{y}(t) &= -(\omega^2 + k)y + kx.\end{aligned}\tag{26}$$

With the initial distributions (A6), (A7), (19) and (20) we can then use the form Eq. (22)

for the transmission coefficient to write

$$\kappa(t) = \int_{-\infty}^{\infty} dv_{y_o} \int_{-\infty}^{\infty} dy_o \int_0^{\infty} dv_{x_o} P(v_{x_o}) P(y_o) P(v_{y_o}) \text{sgn}[x(t; v_{x_o}, y_o, v_{y_o})] \quad (27)$$

where $\text{sgn}[x]$ is the sign function, that is, $\text{sgn}[x] = +1$ if $x > 0$ and -1 if $x < 0$, and $x(t; v_{x_o}, y_o, v_{y_o})$ is the solution of Eqs. (26) with initial conditions v_{x_o} , y_o , v_{y_o} , and $x_o = 0$.

The left panel in Fig. 4 shows two simulations in the energy-diffusion-limited regime along with the results of (27) with (26). The early time agreement in this regime is clearly excellent, as seen in the detail inset. Note that both simulations exhibit the same early-time behavior, even though the value of γ is very different for the two cases (and not particularly “small” in one of the two cases). Clearly, in this regime the values of k and ω^2 determine the early time behavior of the transmission coefficient.

More importantly for our purposes here, the right panel of Fig. 4 shows similar early-time agreement between the stair-like numerical results and the approximation. The agreement extends through the first plateau. Note that the approximation captures the (slightly) non-monotonic behavior of the simulation results. The agreement between the two curves provides the basis for our analysis of the stair-like regime in the next section.

6 The Stair-like Regime

We saw in Sec. 4 that the stair-like regime is achieved when γ and ω^2 are small and the temperature is low. The main feature of this new behavior is that the transmission coefficient shows progressive decays connected by plateaus. The length of the plateaus (determined by a time period that we call T_κ), the depths of the decays, and all the characteristics that define this regime depend on the values of the parameters, principally k . Our understanding of this regime is based on argumentation that relies mainly on the extended system, although some of the arguments can easily be translated to the language of the reduced scheme.

6.1 Trajectories

A particularly helpful view of the process is gained by looking at explicit trajectories, as illustrated in Fig. 5. The solid trajectory $x(t)$ in the left panel illustrates the typical repeated recrossings in the low dissipation energy-diffusion-limited regime. The dotted curves correspond to two typical trajectories in the non-adiabatic regime. Trajectories in this regime almost never recross the barrier. Those that do recross the barrier do so at short times (before straying far from $x = 0$), and typically do so only once. These trajectories reinforce the idea that in this regime particles are quickly trapped in one well or the other due to the high dissipation. As seen in the right panel of Fig. 5, the trajectories in the stair-like regime are considerably more complex – this complexity distinguishes the stair-like dynamics from the other regimes. For example, in this new regime one finds x -particles that remain localized over one well (even though they have sufficient energy to cross the barrier) and that after circling there several times may suddenly recross the barrier. This behavior is not found in any other regime studied so far.

Studying additional x -trajectories besides those shown explicitly in the right panel of Fig. 5 leads to the realization of a number of important points. First, we note that

- the x -particles cross the barrier only at certain specific times.

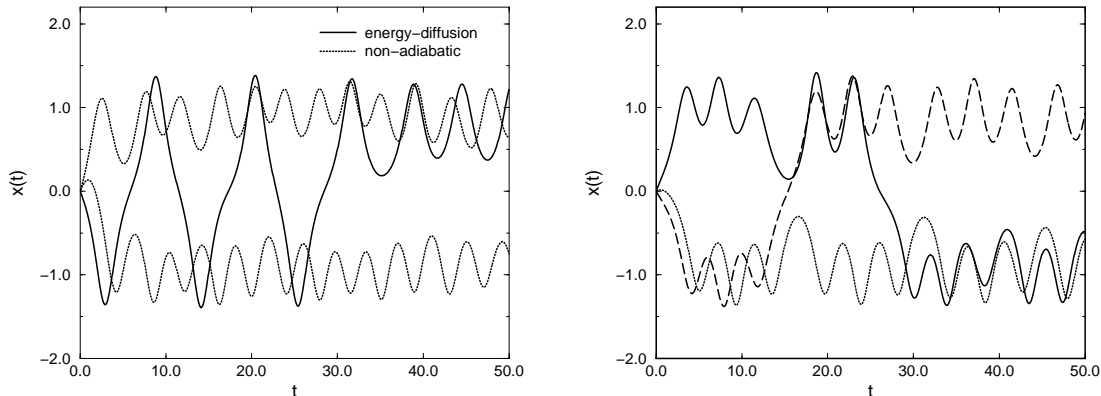


Figure 5: Several typical trajectories of x for different regimes in the oscillatory friction problem. The parameters are those of Fig. 3. Solid curve in left panel: energy-diffusion-limited regime, clearly showing repeated recrossings. Dotted curves in left panel: two examples of non-adiabatic behavior. Right panel: several trajectories associated with the stair-like regime.

For our typical parameters, these times are $t = 10, 16, 25, 31$ and 40 (approximately), which coincide with the decay times T_κ for the associated $\kappa(t)$ in Fig. 3. Moreover, since we are working with low temperatures, the energy of the x -particles is typically not large enough to recross the barrier many times. Actually, we have observed that

- most of the x -particles that cross the barrier do it only once.

Indeed, only about 1% of the particles show multiple recrossings in our typical example. The fact that most particles do not return to their original well once they have crossed the barrier leads to

- steps rather than oscillations.

On the other hand, small friction leads to very slow energy loss, and it is for this reason that

- even at long times crossing the barrier is still possible.

This combination of features characteristic of the energy-diffusion-limited and non-adiabatic regimes ultimately leads to the

- appearance of successive steps and plateaus.

At this point there are two obvious questions about this regime: i) Why do we see decays only at fairly sharply defined specific times and what are these times? In other words, how is the period T_κ determined? ii) What determines the depth of each decay? The answers to these and other questions are given in the following subsections by considering the effects of varying the parameters of our model.

However, before going ahead, we should first understand how an x -particle can be trapped in one well in spite of having enough energy to cross the barrier, as well as how an

x -particle can cross the barrier seemingly without having enough energy to do it. The reason for both strange situations is that the behavior of the x -particles may depend strongly on that of their associated y -oscillators. A given x -particle with energy greater than the barrier height can be “trapped” in one well because each time it goes toward the barrier its coupled oscillator pulls it back. Conversely, a given x -particle with apparently insufficient energy can cross the barrier by being pulled by its y oscillator. Thus, the coupling between x and y may determine the times at which the particles cross the barrier and therefore the times for the decays of $\kappa(t)$.

6.2 Dependence on k

To deduce the role of the coupling constant k , we depart from our typical value ($k = 0.3$) and consider the trajectories for two cases on either side of this value but that still essentially preserve the stair-like behavior. We call them the large- k case ($k = 0.5$) and the small- k case ($k = 0.1$). The parameter k determines the extent to which x and y particle dynamics are in synchrony.

Since $\kappa(t)$ contains information averaged over ensembles of particles, we are interested in the average trajectories of both x and y coordinates. We thus plot $\langle x(t) \rangle$ and $\langle y(t) \rangle$, where $\langle \dots \rangle$ here means an average over all the particles that are in the right well ($x > 0$) at each given time. Fig. 6 shows averaged trajectories for the small- k (left panel) and large- k (right panel) cases.

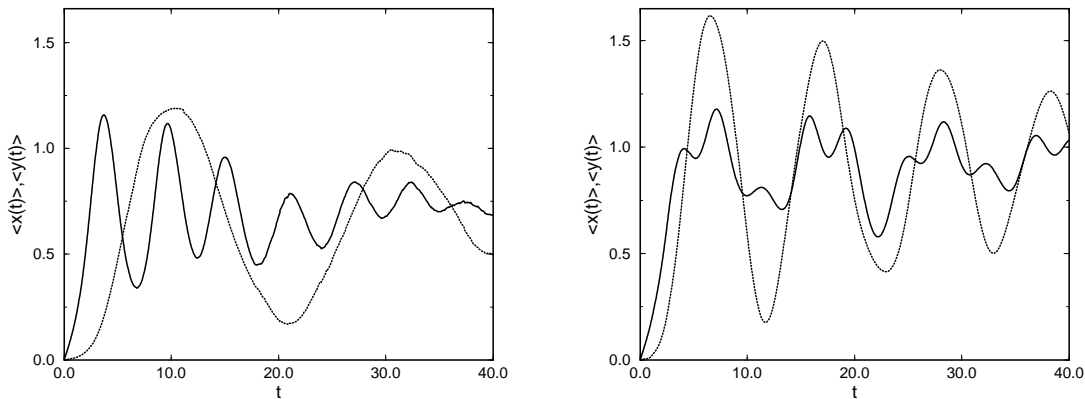


Figure 6: Left panel: $\langle x(t) \rangle$ (solid curve) and $\langle y(t) \rangle$ (dotted curve) for the small- k case. Right panel: $\langle x(t) \rangle$ (solid curve) and $\langle y(t) \rangle$ (dotted curve) for the large- k case.

For the small- k case we readily observe that the motion of $x(t)$ and $y(t)$ are essentially uncorrelated. Each dynamics proceeds with a different principal frequency of oscillation. A Fourier analysis of the trajectories reveals that the peak frequency for $x(t)$ is 1.022 while that of $y(t)$ is 0.306. These frequencies can be associated with two characteristic frequencies of our problem. That of $x(t)$ corresponds to the frequency of the particle in the bistable potential, namely $1.022 \approx 2\pi/T_{semi}$, where T_{semi} is roughly the average semiorbit time for an ensemble of particles above the barrier in the double-well potential. In Ref. [11] we have shown that the semiorbit time for a particle at an energy ε above the barrier is $t_\varepsilon = \ln(16/\varepsilon) + O(\varepsilon \ln \varepsilon)$. An average of this time over a thermal distribution then directly

yields $T_{semi} \approx 3.35 \dots - \ln k_B T$. The frequency of $y(t)$, on the other hand, coincides with the frequency of $\Gamma(t)$, namely $0.306 \approx \Omega \approx \sqrt{k + \omega^2}$. This frequency characterizes the motion of $y(t)$ in the second equation for the extended system, Eq. (9), when the coupling contribution is neglected [see also Eq. (26)]. The x -particles can cross the barrier with frequency $2\pi/T_{semi}$ since they do not care where their associated y -particles are. Thus in this weakly coupled regime

$$T_\kappa \approx T_{semi} \approx 3.35 \dots - \ln k_B T. \quad (28)$$

The large- k case exhibits a different behavior. In this case $x(t)$ and $y(t)$ are essentially synchronized. We see in Fig. 6 that $x(t)$ has two characteristic periods: a shorter one associated with motion in the bistable potential ($2\pi/T_{semi}$) and a longer one that matches that of $y(t)$. The frequency of the latter is 0.624 and coincides with $\sqrt{k + \omega^2} \approx \sqrt{k}$. Thus, the motion of x is now dominated by the dynamics of its coupled oscillator. The consequence of the strong coupling is that now

$$T_\kappa \approx \frac{2\pi}{\Omega} \approx \frac{2\pi}{\sqrt{k}}. \quad (29)$$

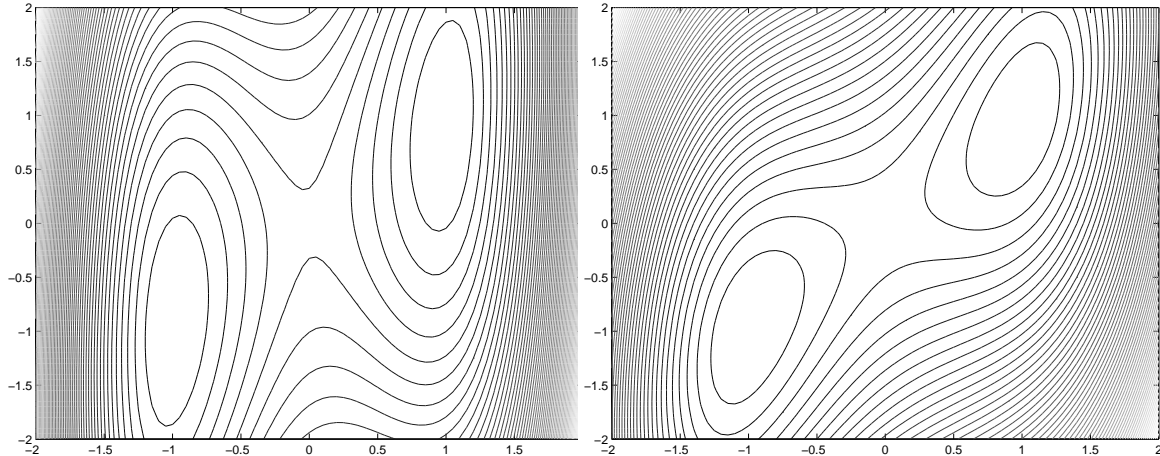


Figure 7: Surface contours for the potential $V(x, y)$ for the small- k (left panel, $k = 0.1$) and large- k (right panel, $k = 0.5$) cases. The coordinates x and y are represented along the horizontal and vertical axes respectively.

These ideas can be further supported by considering the two-variable potential, Eq. (7), drawn in contour form in Fig. 7 for the small- k (left panel) and large- k (right panel) cases. These plots clearly illustrate the correlations between x and y (or the lack thereof). When the system is in one of the two two-dimensional wells, x and y remain more tightly bound in the large- k case than in the small- k case. In particular, when k is small the y -particle can move away from x even when the system has already fallen into one well.

Further, consider the likely pathways followed by the system as it crosses, say, from the right to the left. In the small- k case the likely path is for y to decrease first (perhaps even to negative values), followed by a change of x from $x > 0$ to $x < 0$. On the other hand, in the large- k case it is easier for x to first move from $x > 0$ to $x < 0$ to be followed by y . Therefore, in the large- k case the crossing rate is determined by the frequency of $y(t)$ so

that $T_\kappa \approx 2\pi/\sqrt{k}$; in the small- k case the crossing rate is limited by the motion of $x(t)$ and hence $T_\kappa \approx T_{semi}$.

Figure 8 shows the time-dependent transmission coefficient for the two cases. The times $T_\kappa \approx 7.55$ (small- k case) and $T_\kappa \approx 10$ (large- k case) obtained from the above arguments are consistent with the steps in the figure (measured from mid-point to mid-point), most clearly in the length of the first step.

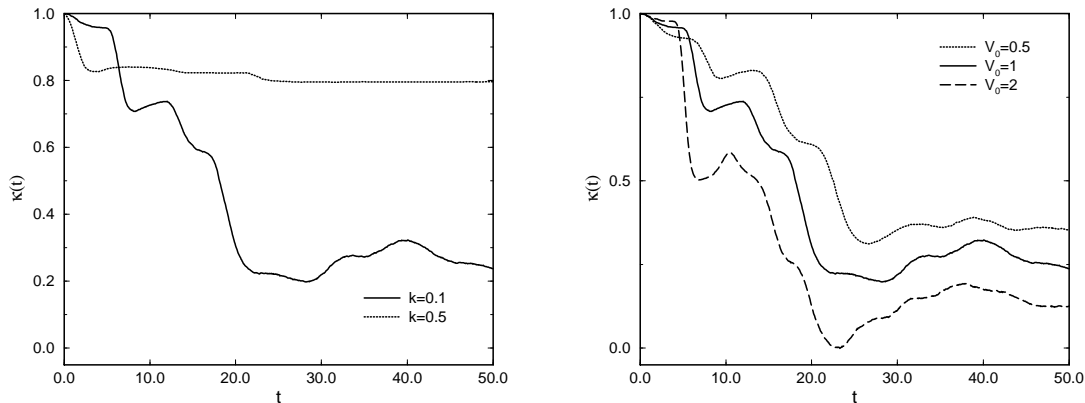


Figure 8: Left panel: $\kappa(t)$ for the small- k and large- k cases discussed in the text. Right panel: Transmission coefficient for the small- k case for three different barrier heights. The solid curve is the same as the small- k case in the left panel.

In addition to the step period differences, the left panel in Fig. 8 illustrates the k -dependence of the depths of the steps in the stair-like transmission coefficient. The steps are clearly deeper when k is small. The reason for this is that the total system loses energy by dissipation only through the y coordinate. Although both cases in the figure correspond to the same value of γ , the x -particles can retain energy for a longer time when k is small. This allows more x -particles to cross the barrier, and it allows them to do so at later times. The deeper and more numerous clear steps in the small- k case are a direct manifestation of these features.

Two further points should be noted. One is the symmetry of the semiorbit time t_ε with respect to ε . That is, the semiorbit time of a particle with an energy ε *above* the barrier is the same as the orbit time of a particle with energy ε *below* the barrier (for small ε). This symmetry is important because it allows particles to remain in synchrony; otherwise the steps in $\kappa(t)$ would be blurred. The other point is the dependence of $\kappa(t)$ and consequently of the period T_κ on barrier height. In general, $t_\varepsilon \approx V_0^{-1/2} \ln(16V_0/\varepsilon)$ (which reduces to our previous expression when $V_0 = 1$), and an average of t_ε over a thermal distribution of particles above the barrier yields the generalization of Eq. (28)

$$T_\kappa \approx \frac{1}{V_0^{1/2}} (\ln 16V_0 + 0.5772\dots - \ln k_B T). \quad (30)$$

The right panel in Fig. 8 shows the transmission coefficient in the small- k case for three values of the barrier height. The corresponding period estimates for $T_\kappa(V_0)$ obtained from Eq. (30) are $T_\kappa(0.5) = 9.70$, $T_\kappa(1.0) = 7.55$, and $T_\kappa(2.0) = 5.83$. These decreasing periods

with increasing barrier height are clearly consistent with the numerical results.

6.3 Dependence on γ

We have seen that successive steps in the transmission coefficient arise because the particles lose their energy slowly. This requires γ to be small – but not too small (cf. below). Indeed, if γ is decreased we expect particles to lose their energy even more slowly, which leads to a larger number of deeper steps. However, as γ continues to decrease we expect to begin to see particles that cross the barrier more than once before becoming trapped. This leads to oscillations in $\kappa(t)$ and, eventually, to energy-diffusion-limited behavior. Deeper steps and the first appearance of small oscillations with decreasing γ are clearly evident in the left panel of Fig.9.

Conversely, if γ is increased, particles lose their energy more rapidly, and fewer particles cross the barrier at all; those that do so cross at most once. In this case, as seen in Fig. 9, the steps are less deep and almost disappear at long times. Indeed, the limit of the stair-like behavior with increasing γ is the monotonic non-adiabatic regime, where only a few particles cross the barrier and they do so at very short times.

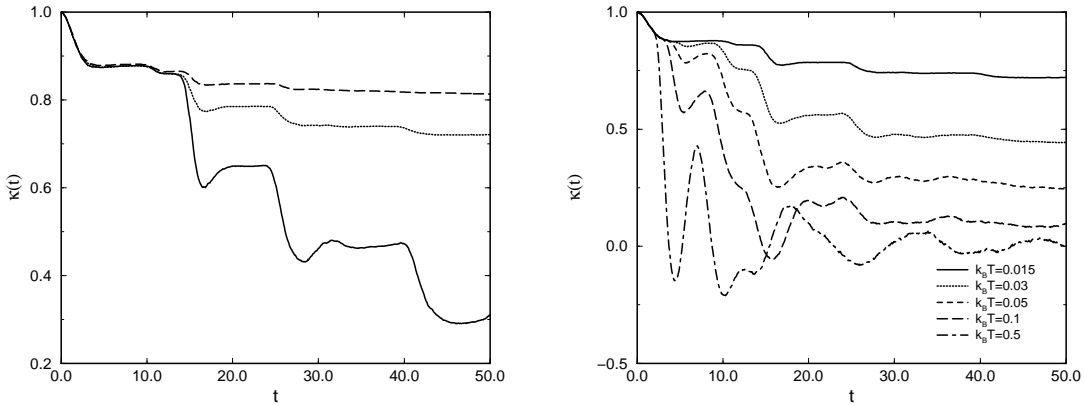


Figure 9: Left panel: dependence of the stair-like transmission coefficient on the dissipation parameter γ . The parameters are otherwise those of our typical example in Fig. 3: $\omega^2 = 0.01$, $k = 0.3$, $k_B T = 0.015$. Dotted curve: $\gamma = 0.05$; solid curve: $\gamma = 0.01$; dashed curve: $\gamma = 0.1$. Right panel: dependence of the stair-like transmission coefficient on temperature; the other parameters are those of Fig. 3.

6.4 Dependence on $k_B T$

Finally, we consider the temperature dependence of the transmission coefficient in the stair-like regime. As temperature is increased, all else remaining the same, there is a greater number of more energetic x -particles above the barrier. Two aspects of their behavior dominate the resulting transmission coefficient. One is that the particles now have a greater range of semiorbit times t_ε ; the other, more important, effect is that particles are now sufficiently energetic that they can recross the barrier more than once. These are precisely the features that lead to the typical oscillatory behavior of the transmission coefficient

in the energy-diffusion-limited regime, and it is towards this behavior that the stair-like regime tends with increasing temperature. The right panel in Fig. 9 shows this progression very clearly: the highest temperature results look very much like the earlier curves for the energy-diffusion-limited case. We should note the deeper first decay in the $k_B T = 0.5$ curve than observed in our earlier illustrations. This is due to the fact that here we have chosen ω^2 to be very small (a requirement for the stair-like regime). This causes the initial thermal distribution of $y(0)$ to pull back x -particles more effectively than in our earlier example, and this in turn leads to the deeper decay.

6.5 Arguments in the Reduced System

Since the extended [Eq. (9)] and reduced [Eq. (1)] systems are entirely equivalent, it is of course possible to explain the new stair-like regime in terms of quantities and equations associated with the reduced representation. It is perhaps somewhat more cumbersome and less transparent, but the extended representation analysis offers a helpful guide. For example, it is useful to realize that a “negative friction” [i.e., a negative value of the memory kernel in Eq. (1)] in the reduced representation is associated with the situation where in the extended system the y -coordinate pulls the x -particle in the direction of \dot{x} .

To explain the different decay periods T_κ in the reduced representation we note that the memory kernel $\Gamma(t)$ is proportional to k^2 and the random force $F(t)$ is proportional to k . To cross the barrier, an x -particle must be moving towards $x = 0$. When k is small, the dynamics of x as it moves in the barrier region is thus dominated by the bistable potential $V_{eff}(x)$. In particular, the decay periods in $\kappa(t)$ are determined by the frequency of the particles moving in the bistable potential with energies slightly larger and slightly smaller than the barrier height, which directly leads again to the earlier estimate $T_\kappa = T_{semi}$ [cf. Eq. (28)]. The slow dissipation of x -energy associated with small k allows for many deep steps in $\kappa(t)$.

As k increases, the bistable potential becomes relatively less important and the first and third terms on the right of Eq. (1) increasingly dominate the dynamics of $x(t)$. The steps in $\kappa(t)$ then acquire the period $T_\kappa \approx 2\pi/\Omega \approx 2\pi/\sqrt{k}$ associated with the friction kernel. The more rapid dissipation of x -energy associated with larger k leads to a small number of shallow steps.

The dependence on γ in this representations is quite clear. When γ increases, the memory kernel decays more rapidly and the oscillations in $\Gamma(t)$ become irrelevant, thus leading to non-adiabatic behavior of $\kappa(t)$. Decreasing γ , on the other hand, leads to pronounced oscillations (and at times negative values) of $\Gamma(t)$. As a result, even particles that start out with energies too low to cross the barrier early may do so at a later time, thus explaining the step structure of $\kappa(t)$. The temperature dependence can also be understood: for a given (low) γ , increasing the temperature leads to a greater number of particles above the barrier that can recross more than once before becoming trapped. The steps then become oscillations and the energy-diffusion-limited behavior is recovered.

7 Conclusions

In this work we have analyzed the time dependent transmission coefficient for the capture of a particle in one or the other well of a bistable potential as described by the generalized Kramers equation Eq. (1) with an oscillatory memory kernel. The time dependence of the transmission coefficient depends sensitively on the parameters of the model. The equivalence

of this model to an “extended system” wherein the reaction coordinate is linearly coupled to a nonreactive coordinate which is in turn coupled to a heat bath, Eq. (9), facilitates the understanding of the various time dependences that are observed.

The different behaviors observed for the transmission coefficient in various parameter regimes are summarized in Fig. 3. The non-adiabatic (monotonic decay) and energy-diffusion-limited (oscillatory decay) behaviors have been encountered earlier in the classic Kramers problem [11,13,14,16] and in the generalized Kramers problem with an exponential memory kernel [12–14,16]. The non-adiabatic decay is observed when the reaction coordinate loses its energy rapidly, so that particles cross the barrier only at early times and at most once before becoming trapped. The oscillatory behavior is observed when the reaction coordinate loses its energy slowly, thus allowing several recrossings of the barrier before trapping. These regimes are associated with parameter values that suppress the oscillations of the memory kernel. There is a third behavior observed with exponential friction, the caging regime, which is not observed with an oscillatory memory friction.

The third behavior shown in Fig. 3, which consists of a stair-like decay of the transmission coefficient, is peculiar to the oscillatory memory friction and occurs when the oscillations in the memory kernel are pronounced. This behavior is observed when particles cross the barrier at most once, but not necessarily at early times. In turn, this can be explained by the fact that particles that at one time may not have enough energy to cross the barrier may acquire sufficient energy to do so later via their coupling to the nonreactive coordinate (or, equivalently, when the oscillations in the memory kernel periodically lead to negative values of the kernel). Although the particles cross the barrier at most once, and not necessarily at early times, the crossing events can only occur at fairly sharply defined time intervals that we call T_κ . Hence the appearance of fairly sharp steps in the transmission coefficient. We explain in detail the conditions that lead to the stair-like behavior, the way in which the step time T_κ and the step depths depend on the parameters of the system, and the way in which this behavior tends to the energy-diffusion-limited or non-adiabatic cases as parameters are modified.

If there were no barrier crossings at all in the Kramers problem, the transmission coefficient would be unity. Single barrier crossings only at early times lead to monotonic decay of the transmission coefficient. Single recrossings that are possible only at specified time intervals T_κ lead to the new stair-like regime. Multiple recrossings lead to oscillatory behavior. The time dependence of the transmission coefficient clearly provides an interesting mirror for the barrier crossing dynamics of the generalized Kramers problem.

Acknowledgments

One of us (R. R.) gratefully acknowledges the support of this research by the Ministerio de Educación y Cultura through Postdoctoral Grant No. PF-98-46573147. This work was supported in part by the U. S. Department of Energy under Grant No. DE-FG03-86ER13606, and in part by the Comisión Interministerial de Ciencia y Tecnología (Spain) Project No. DGICYT PB96-0241.

A Extended vs Reduced Model

Here we present the analytical details connecting Eqs. (1) and (9). Formal solution of Eq. (9) gives

$$y(t) = \frac{v_{y_0} - y_0 \lambda_2}{\lambda_1 - \lambda_2} e^{\lambda_1 t} + \frac{y_0 \lambda_1 - v_{y_0}}{\lambda_1 - \lambda_2} e^{\lambda_2 t} + \frac{1}{\lambda_1 - \lambda_2} \int_0^t dt' \left(e^{\lambda_1(t-t')} - e^{\lambda_2(t-t')} \right) [kx(t') + f(t')], \quad (\text{A1})$$

where the first two terms on the right hand side correspond to the homogeneous solution that depends on the initial conditions $y(0) \equiv y_0$ and $\dot{y}(0) \equiv v_{y_0}$. The last two terms correspond to the inhomogeneous solution. The term proportional to k leads to the memory friction term and the term containing $f(t')$ is associated with the colored noise in the reduced model. The roots λ_i are

$$\lambda_{1,2} = -\frac{\gamma}{2} \pm \sqrt{\left(\frac{\gamma}{2}\right)^2 - \omega^2 - k}. \quad (\text{A2})$$

Substitution of this formal solution in Eq. (9) and regrouping of terms directly leads to the reduced model (1) with the memory kernel

$$\Gamma(t) = \frac{k^2}{\lambda_2 - \lambda_1} \left(\frac{e^{\lambda_1 t}}{\lambda_1} - \frac{e^{\lambda_2 t}}{\lambda_2} \right). \quad (\text{A3})$$

We also get the explicit form for the effective potential of the reaction coordinate,

$$V_{eff}(x) = V(x) + \frac{1}{2} \frac{\omega^2 k}{\omega^2 + k} x^2. \quad (\text{A4})$$

However, the following extra initial conditions must be fulfilled in order to avoid transient terms in the reduced model:

$$x(0) = 0; \quad \langle v_{y_0} \rangle = \langle y_0 \rangle = 0; \quad \langle v_{y_0}^2 \rangle = k_B T; \quad \langle y_0^2 \rangle = \frac{k_B T}{\omega^2 + k}. \quad (\text{A5})$$

The brackets here indicate averages over initial distributions. The following initial distributions for the solvent coordinate are consistent with these requirements:

$$P(y_0) = \sqrt{\frac{\omega^2 + k}{2\pi k_B T}} \exp\left(-\frac{(\omega^2 + k)y_0^2}{2k_B T}\right) \quad (\text{A6})$$

and

$$P(v_{y_0}) = \frac{1}{\sqrt{2\pi k_B T}} \exp\left(-\frac{v_{y_0}^2}{2k_B T}\right). \quad (\text{A7})$$

The explicit reduction (integration) thus readily leads to the observation that the initial

conditions for y are the thermalized solutions of the homogeneous differential equation

$$\ddot{y} + \gamma\dot{y} + (\omega^2 + k)y = 0. \quad (\text{A8})$$

That is, we must thermalize the solvent coordinate evolving in the combined intrinsic and coupling potential with the reaction coordinate fixed at $x = 0$.

At this point, a distinction should be made between the following two behaviors of the friction kernel. The first is the underdamped case, where the condition

$$\Omega^2 \equiv \omega^2 + k - \left(\frac{\gamma}{2}\right)^2 > 0 \quad (\text{A9})$$

leads to complex values for λ_1 and λ_2 ,

$$\lambda_{1,2} = -\frac{\gamma}{2} \pm i\Omega, \quad (\text{A10})$$

which in turn leads to a trigonometric form for the memory kernel (sometimes called the “trigonometric case”):

$$\Gamma(t) = \frac{k^2}{\omega^2 + k} e^{-\frac{\gamma}{2}t} \left(\frac{\gamma}{2\Omega} \sin \Omega t + \cos \Omega t \right). \quad (\text{A11})$$

The second behavior, the overdamped case, results when

$$\Lambda^2 \equiv \left(\frac{\gamma}{2}\right)^2 - \omega^2 - k \geq 0. \quad (\text{A12})$$

In this case the values of λ_1 and λ_2 are real,

$$\lambda_{1,2} = -\frac{\gamma}{2} \pm \Lambda, \quad (\text{A13})$$

and therefore the memory kernel has a hyperbolic form (sometimes called the “hyperbolic case”):

$$\Gamma(t) = \frac{k^2}{\omega^2 + k} e^{-\frac{\gamma}{2}t} \left(\frac{\gamma}{2\Lambda} \sinh \Lambda t + \cosh \Lambda t \right). \quad (\text{A14})$$

References

- [1] H.A. Kramers, *Physica* **7**, 284 (1940).
- [2] R. F. Grote and J. T. Hynes, *J. Chem. Phys.* **73**, 2715 (1980).
- [3] P. Hanggi, P. Talkner and M. Borkovec, *Rev. Mod. Phys.* **62**, 251 (1990).
- [4] V. I. Melnikov, *Phys. Report* **209**, 1 (1991).
- [5] E. Pollak, in *Activated Barrier Crossing*, eds. P. Hanggi and G. Fleming (World Scientific, Singapore, 1992).
- [6] S. C. Tucker, in *New Trends in Kramers Reaction Rate Theory: Understanding Chemical Reactivity*, eds. P. Talkner and P. Hanggi (Kluwer Academic, Dordrecht, 1995).

- [7] V. I. Melnikov and S. V. Meshkov, *J. Chem. Phys.* **85**, 1018 (1986).
- [8] E. Pollak, H. Grabert and P. Hanggi, *J. Chem. Phys.* **91**, 4073 (1989).
- [9] E. Pollak and P. Talkner, *Phys. Rev. E* **47**, 922 (1993).
- [10] V. I. Melnikov, *Phys. Rev. E* **48**, 3271 (1993).
- [11] J. M. Sancho, A. H. Romero and K. Lindenberg, *J. Chem. Phys.* **109**, 9888 (1998).
- [12] K. Lindenberg, A. H. Romero and J. M. Sancho, to appear in *Physica D*.
- [13] J.A. Montgomery, Jr, D. Chandler, and B. J. Berne, *J. Chem.Phys.* **70**, 4056 (1979).
- [14] D. Borgis and M. Moreau, *Mol. Phys.* **57**, 33 (1986).
- [15] S. Tucker, *J. Chem. Phys.* **101** (1994) 2006; S. K. Reese, S. Tucker, and G. K. Schenter, *J. Chem. Phys.* **102** (1995) 104.
- [16] D. Kohen and D.J. Tannor, *J Chem. Phys.* **103**, 6013 (1995).
- [17] J. E. Straub and B.J. Berne, *J. Chem. Phys.* **83**, 1138 (1985).
- [18] J. E. Straub, D.A. Hsu, and B.J. Berne, *J. Phys. Chem.* **89**, 5188 (1985).
- [19] T.C. Gard, *Introduction to Stochastic Differential Equations*, Marcel Dekker, Vol.114 of *Monographs and Textbooks in Pure and Applied Mathematics* (1987).
- [20] R. Toral, in *Computational Field Theory and Pattern Formation*, 3rd Granada Lectures in Computational Physics, Lecture Notes in Physics Vol. 448 (Springer Verlag, Berlin, 1995).